Journal of the Serbian Chemical Society
JSCS-info@shd.org.rs • www.shd.org.rs/JSCS
J. Serb. Chem. Soc. 81 (2) 103–123 (2016) UDC 547.978.1–114+542.913:576+615.9:004.2
JSCS–4831 *Original scientific paper*

Synthesis, cytotoxicity and computational study of novel protoberberine derivatives

MILENA R. SIMIĆ[1]*, ANA B. DAMJANOVIĆ[2], MARKO D. KALINIĆ[3#], GORDANA D. TASIĆ[1], SLAVICA M. ERIĆ[3], JELENA A. ANTIĆ-STANKOVIĆ[4] and VLADIMIR M. SAVIĆ[1]**[#]

[1]*University of Belgrade, Faculty of Pharmacy, Department of Organic Chemistry, Vojvode Stepe 450, 11221 Belgrade, Serbia,* [2]*Institute of Oncology and Radiology, Department of Experimental Oncology, Pasterova 14, 11000 Belgrade, Serbia,* [3]*University of Belgrade, Faculty of Pharmacy, Department of Pharmaceutical Chemistry, Vojvode Stepe 450, 11221 Belgrade, Serbia and* [4]*University of Belgrade, Faculty of Pharmacy, Department of Immunology and Microbiology, Vojvode Stepe 450, 11221 Belgrade, Serbia*

(Received 25 May, revised 19 October, accepted 26 October 2015)

Abstract: A novel and efficient synthetic route was developed for the preparation of protoberberine derivatives. A methodology, designed primarily to control the substitution patterns on the terminal rings, was used to access a small array of these compounds. An initial biological profiling suggested an anticancer potential of the synthesised derivatives, while structure-based target fishing identified their potential targets and established a rational basis for further structural modifications. Although the activities need further improvement, the study demonstrated that the described approach may be useful in the discovery of novel lead compounds.

Keywords: cytotoxic properties; protoberberine; privileged structure; synthesis; target fishing.

INTRODUCTION

Natural products represent a valuable source of biologically active compounds and have played an important role in the drug discovery process.[1–9] In recent years, their influence on the research in pharmaceutical companies has arguably been on the decline mainly due to the advent of combinatorial chemistry and the expectations that it may secure access to a large number of new lead compounds.[8] Even so, in the period between 2000 and 2006, a total of 26 new natural products or natural products-derived drugs were launched worldwide with

*,** Corresponding authors. E-mail: (*)milena@pharmacy.bg.ac.rs, (**)vladimir.savic@pharmacy.bg.ac.rs
[#] Serbian Chemical Society member.
doi: 10.2298/JSC150525090S

many more being in clinical trials, suggesting that naturally occurring compounds continue to play a prominent role in drug discovery.[10] Undoubtedly useful as a starting point in the finding of new therapeutics, they also impose some limitations as a result of often insufficient availability and complex structural requirements. Therefore, the development of similar analogues with comparative biological properties is highly desirable and may provide access to a chemical space not approachable by convenient combinatorial synthesis.[11,12] In recent years, various tools have been developed in order to facilitate the process of creating collections of natural products-derived compounds.[13] Our interest in natural products inspired the search for new anticancer derivatives, which led to the study of polycyclic protoberberines.[14–16] This class of compounds shows a wide range of biological activities including anticancer properties, which are associated with several mechanistic pathways. It was proposed that they bind to the DNA B-form by partial intercalation, showing AT base pair specificity.[17] In addition, they may interact with polyriboadenylic acid, an important factor for the stability and maturation of mRNA.[18] Some studies also suggested that protoberberines inhibit topoisomerase through stabilisation of the enzyme–DNA complex.[19,20] The most frequent protoberberinic structures (Fig. 1, represented by pseudopalmatine, xylopinine and gusanlung D) are typically characterised by a tetracyclic core in which rings A and D are aromatic while ring C diverges in its oxidation state.

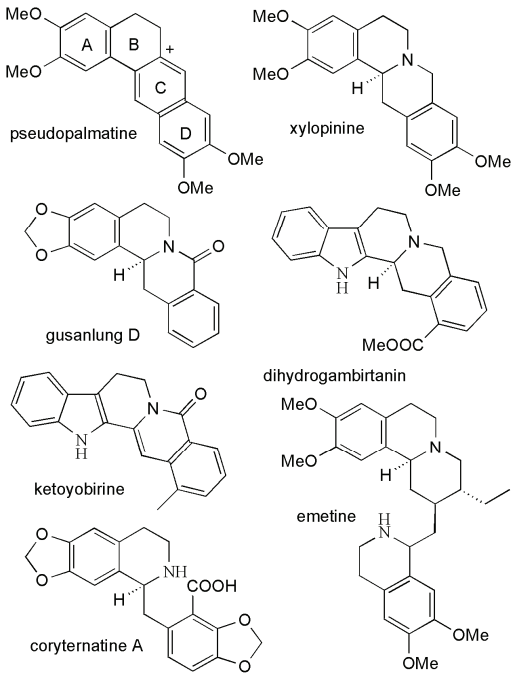

Fig. 1. Protoberberines and related natural products.

The substitution patterns usually present in these compounds are the result of the oxygenation of rings A and D. Related to protoberberins are dihydrogambirtannine and ketoyobyrine while some similarities exist with the structures of emetinoides and benzylisoquinolines as well (Fig. 1).[21–24] The present study to find new classes of compounds with anticancer potential was initiated with hopes to enter a new chemical space defined by these natural products and the initial results will be discussed further in this text.

RESULTS AND DISCUSSION

Chemistry

Analysis of the structural properties of compounds outlined in Fig. 1 and related derivatives led to two associated scaffolds, **1** and **2** (Fig. 2). Their calculated volumes are 155 and 192 Å^3, respectively, which, compared with the average calculated volumes of protein cavities, generally leave enough space for their wider functionalisation.[25]

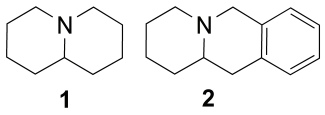

1 **2**

Fig. 2. Protoberberine-based scaffolds.

Although all compounds could be considered as derivatives of these two, the oxidation level and substitution patterns of the terminal rings vary. In order to increase synthetic efficiency and potentially to expand the chemical space later *via* diversity orientated synthesis, it was essential to develop a flexible route that will diverge to various derivatives *via* a common intermediate. These criteria were fulfilled by the synthetic route outlined in Scheme 1.[26] Quaternisation of pyridine with allyl bromide (**3a**) afforded the pyridinium salt **4** in a good yield. Further reaction of **4** with Grignard reagent furnished, as expected, two regioisomeric products **5** and **6**, which were subsequently reduced using $NaBH_3CN$ to eliminate the labile enamine functionality.[27–29] At this stage the regioisomeric products were separated and compound **7** was submitted to typical conditions for the Heck reaction.[30,31] The expected diene **9** was obtained in 26 % yield and set the stage for key transformations expected to lead to the target compounds. Diels–Alder reaction of diene **9** with dimethyl acetylenedicarboxylate (DMAD) afforded the tricyclic cycloadduct **10**.[32–34] After some experimentation, it was found that careful oxidation of **10** produced both the tetrahydro- and oxo-type skeleton, **11** and **12**, respectively, found in the above-mentioned natural products.[35–37] Thus, by developing this route, three classes of natural compound-related derivatives based on scaffold **1**/**2**, type **10**–**12**, could be prepared.

Next, this synthetic route was applied to the preparation of tetrahydro- and oxoprotoberberine derived compounds (Scheme 2). The synthesis of diene **17**

was initiated by the alkylation of isoquinoline **13** followed by the same reaction sequence as outlined in Scheme 1. Diene **17** proved to be sufficiently reactive in boiling toluene to afford the cycloadducts **18** with either a mono- or bis-activated alkyne. Exploration of the oxidative processes secured access to both tetrahydro- and oxoprotoberberine derivatives. Careful control of the reaction conditions, primarily a lower amount of MnO_2, produced tetrahydroprotoberberines **19**, while larger quantities of the oxidant afforded the oxo derivatives **20**. Monitoring the reaction by thin layer chromatography (TLC) was important because the oxo compound **20** was formed *via* further oxidation of the initially formed tetrahydro derivative **19**. This was facilitated by the different, characteristic TLC appearance of these compounds (orange–red for **19** *vs*. grey–blue for **20**).

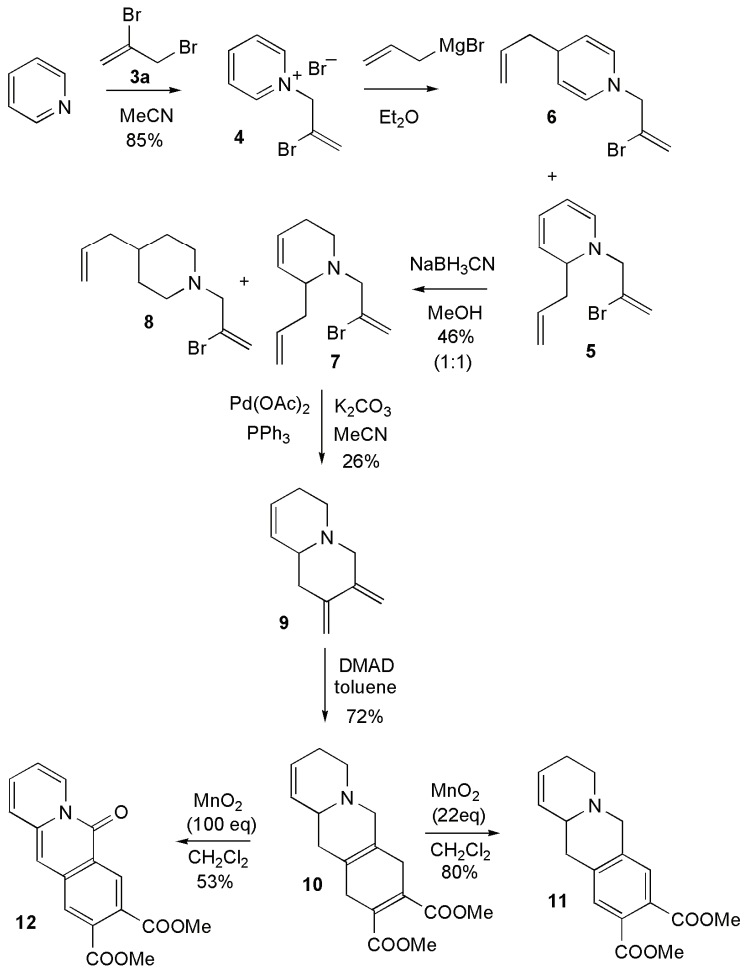

Scheme 1. Synthesis of pyridine derivatives.

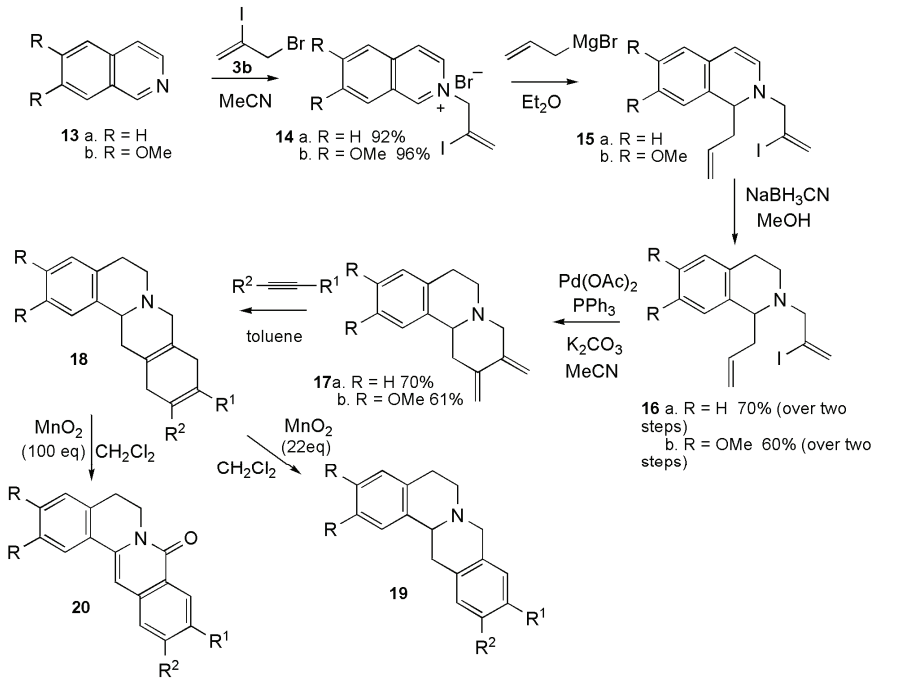

entry	cycloadduct **18**	tetrahydroprotoberberine **19**	oxoprotoberberine **20**
a	**18a** 90%	**19a** 63%	**20a** 70%
b	**18b**[a]	**19b** 36%	**20b** 45%
c	**18c** 80%	**19c** 78%	**20c** 50%

[a] Regioisomeric **18b'** was also isolated (see experimental)

Scheme 2. Synthesis of protoberberine derivatives.

Finally, dihydro-*β*-carboline **21** was annulated using the same reaction sequence to produce compound **26**, possessing a dihydrogambirtanin core, and oxo derivative **27**, with a ketoyobirine structure, *via* the common intermediate **25** (Scheme 3).

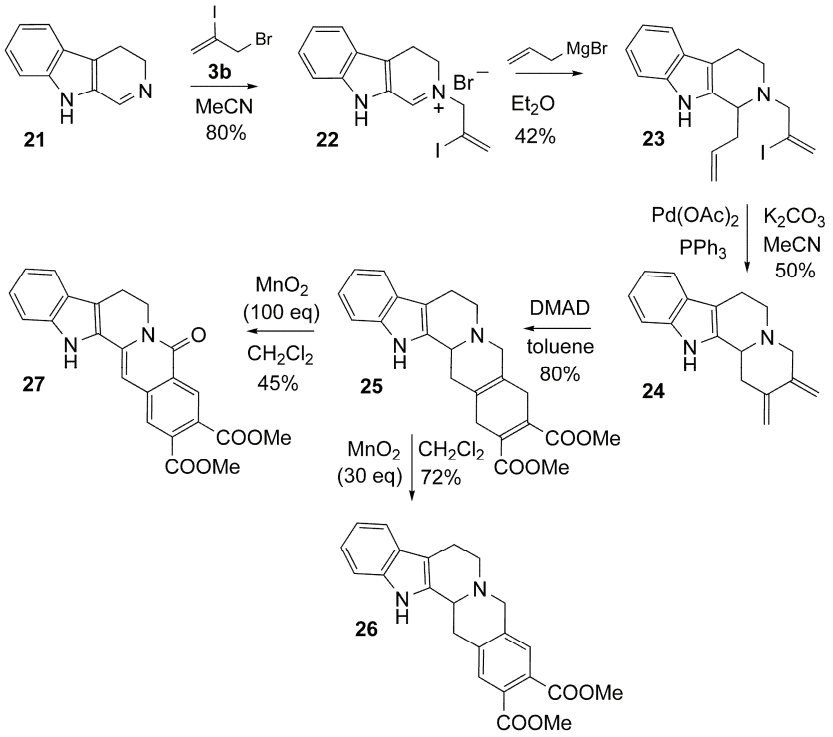

Scheme 3. Synthesis of dihydrogambirtanin and ketoyobirine derivatives.

The developed synthetic route provided in a straightforward manner access to several classes of protoberberine-like compounds derived from pyridine, isoquinoline and 3,4-dihydro-*β*-carboline. Importantly, it has the potential to diversify further the target structures *via* functionalization of the common diene intermediate.

Biology

The *in vitro* cytotoxicity of selected synthesised compounds was studied against three human cancer cell lines, human cervix adenocarcinoma (HeLa), human melanoma (Fem-x) and human chronic myelogenous leukaemia (K562). For this purpose, a tetrazolium-based colorimetric assay (MTT) was employed, while the activity of the tested compounds was compared with that of cisplatin as

a positive control (Table I). The results of the *in vitro* cytotoxic activity are expressed as IC_{50} in μM.

TABLE I. Cytotoxicity of the synthesised protoberberine derivatives

Entry	Compound	FemX[a]	HeLa[a]	K562[a]
a	**25**	81.8±9.3	68.5±5.3	28.8±9.7
b	**18a**	88.5±9.0	82.9±12.4	53.3±2.4
c	**20a**[b]	178.2±2.0	134.5±7.0	101.2±11.2
d	**20a**[c]	>200	>200	>193
e	**20b**[b]	187.7±8.9	120.8±11.8	85.9±21.0
f	**20b**[c]	>179	>179	>165
g	**18b**	65.5±0.5	38.1±8.9	24.7±0.2
h	**18c**	157.9±2.4	152.1±7.6	87.1±14.9
i	**20c**	188.1±13.4	92.8±6.3	85.9±1.1
j	**19a**	86.7±8.5	93.8±3.6	52.4±7.4
k	**11**	178.2±12.6	>200	104.4±7.6
l	**26**	136.7±8.3	48.8±3.6	36.1±10.1
m	**19c**	150.7±14.5	133.3±10.2	46.7±5.9
n	**19b**	172.6±10.0	188.4±0.5	67.7±12.3
o	cisplatin	11.1±6.9	6.4±0.2	6.3±0.7

[a]The results are presented as mean IC_{50} ± standard deviation, μM; [b]compounds crystallised upon preparation of the sample; [c]compounds crystallised upon preparation of the sample and the shown results were obtained with a solution, after filtration and separation of the crystals

Amongst the studied cell lines, K562 was shown to be the most sensitive towards the tested compounds with derivatives **18b** and **25** being the most active (Table I, K562: entries g and a). The HeLa cell line was less responsive and two compounds, **18b** and **26** (Table I, HeLa: entries g and l), exhibited better biological profiles than the others. Tested heterocycles demonstrated lowest activity against the FemX cell line while compound **18b** (Table I, FemX: entry g) was again the most active one. The narrow number of compounds prepared for this initial investigation cannot allow detailed structure–activity relationship studies but some trends could be identified, in particular for the most sensitive K562 cell line. In general, derivatives possessing an amide functionality in the oxoprotoberberine skeleton, (Table I, **20a**–**c**) were less active than the corresponding tertiary amines (Table I, *e.g.*, **18b**, **19a**, **19c**, **25**, **26**) and this trend was general for all three cell lines.

This might suggest that basic properties contribute to a better biological profile, either *via* influencing the physicochemical features of the compounds or due to specific interactions with the target molecules. Regarding the oxidation state of the terminal ring, which was either in the cyclohexadiene or the benzene form, no significant differences between these derivatives were observed for some compounds (Table I, **25** *vs*. **26** and **18a** *vs*.**19a**) but not all (Table I, **18b** *vs*. **19b**). Finally, the observed activity of the tested compounds suggested that the least

active are derivatives prepared *via* annulation of the pyridine ring, while isoquinoline and β-carboline derivatives showed comparable properties. In order to gain insight into the mechanism of action of the active compounds, further their effects on the cell cycle were explored. The experiments were realised with compounds **19a**, **25** and **26** on the HeLa cells. The cells were treated for 24 h with the studied derivatives and were then stained with propidium iodide (PI) followed by flow cytometry analysis. Representative cell-cycle distributions of HeLa cells incubated in the absence or presence of **19a**, **25** and **26** for 24 h are shown in Fig. 3. The obtained DNA histogram indicated that treatment with IC_{50} or $2\times IC_{50}$ for 24 h led to a significant increase in the number of sub-G1 phase cells and a decrease in the number of G1 and G2/M cells after treatment with all three compounds. A further study involved the acridine orange (AO)/ethidium bromide (EB) double staining assay to determine the mode of HeLa cells death induced by **19a**, **25** and **26**.

Microphotographs of the treated cells showed that the tested compounds induced chromatin condensation (indicated by the arrows in Fig. 4b–d) and nuclear fragmentations (indicated by arrowhead in Fig. 4b–d) processes considered to be hallmarks of apoptosis.[38] Based on these results, it would be appropriate to propose that the promotion of apoptosis is the likely mode of action of synthesised protoberberine compounds.

Computational chemistry

The initial biological studies of the compounds outlined in Table I suggest that they possess antiproliferative potential, but it is obvious that further structural modifications are necessary in order to optimize their properties. In order to be able to make rational structural variations, a computational study of these heterocycles was embarked on with the aim of defining their potential target biomolecules. Structure-based target fishing can provide a rational basis for generating hypotheses regarding the mechanism of action of compounds with established biological activity.[39,40] Within the framework of this method, high-throughput molecular docking of the investigated compounds was performed against a set of biomolecules that are known to bind either a cognate ligand or synthetic small molecules. The resulting docking scores were then used to prioritize a smaller number of putative targets under the assumption that those targets yielding higher docking scores are more likely to be genuine targets in biological settings. Despite inherent limitations of the available docking methodologies, this approach was demonstrated as useful in identifying a smaller number of putative targets for further evaluation.[41–46] Since the present aim was to rationalize the observed antiproliferative activities, targets were first prioritized based on the agreement between docking scores and the determined *in vitro* activity. This allowed the utilisation of all the available experimental data, but necessarily assumed that the *in vitro* cytotoxicity reflects on-target efficacy and was not dispro-

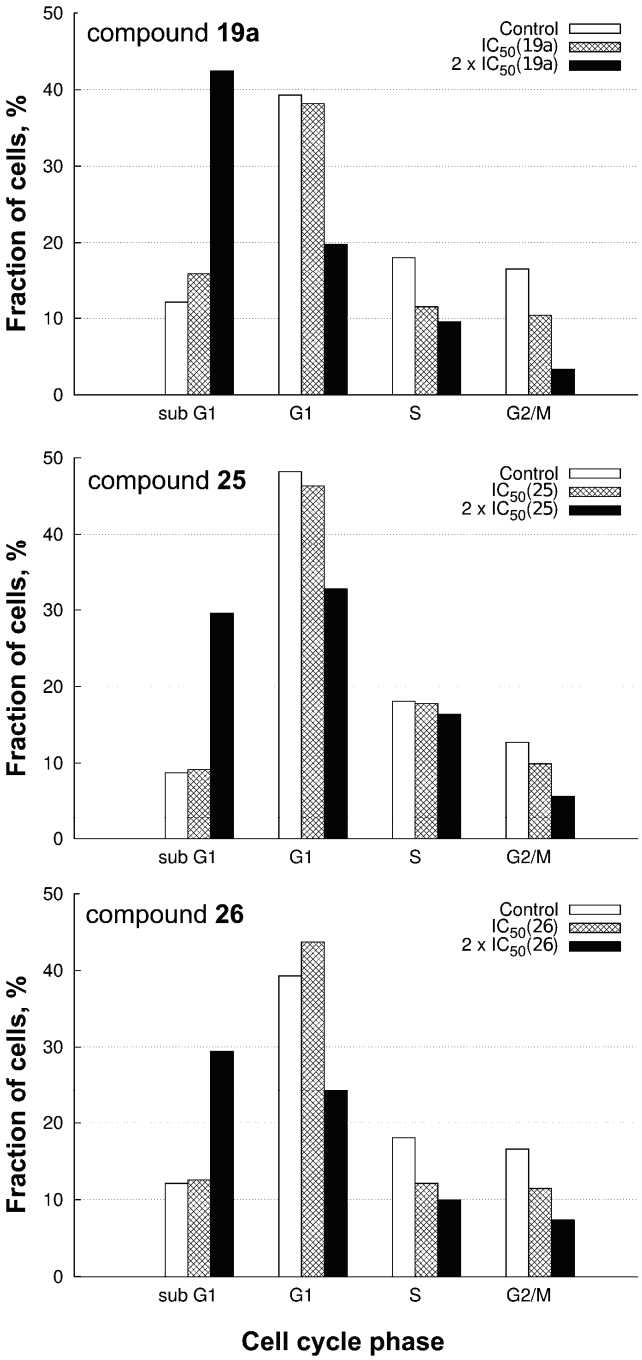

Fig. 3. Cell cycle distribution after 24 h continuous action of compounds **19a**, **25** and **26** on HeLa cells.

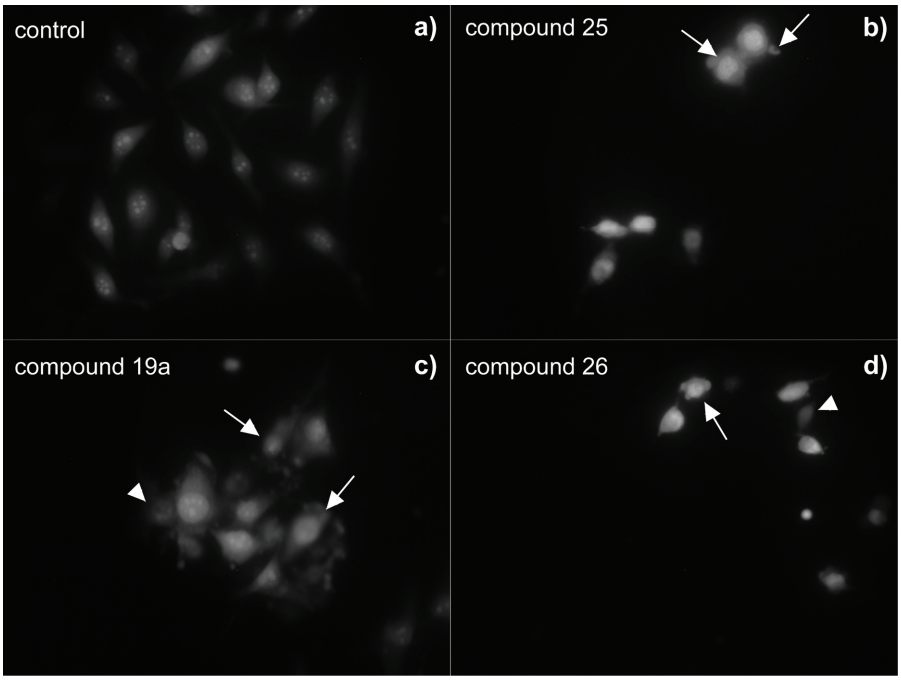

Fig. 4. Induction of apoptosis in HeLa cells by compounds **25**, **19a** and **26**.

portionately limited by other factors, such as permeability or active efflux. In interpreting the results, this assumption was taken into account, especially considering the lower solubilities of **20a** and **20b**. In the second stage of target rank-ordering, it was assumed that the structural similarity and similarities of the observed cell-cycle effects of the studied protoberberines suggested that they shared a common mode of action. Accordingly, targets with higher overall docking scores across all the active protoberberines were considered more likely targets than those with a lower sum of docking scores. Data mining of the obtained matrix of the docking results revealed a number of putative targets, which showed good correlation to the determined IC_{50} values. The ten targets that displayed the best correlations are listed in Table II. For these ten targets, as an additional rank-ordering parameter, sums of docking scores across all the active protoberberines were calculated and are also given in Table II. It should be noted that these sums were derived from normalized docking scores, which comprehensively take into account: *i*) the non-specific contribution of molecular size to docking results,[46,47] *ii*) the differences between the screened protein structures and *iii*) the docking scores of known ligands relative to those of the investigated compounds.

The mean Vina docking scores for the 12 protoberberines at all 10 targets are summarized in Table III.

TABLE II. Summary of the virtual screening results

Target[a] (PDB entry)	K562		HeLa		FemX	
	R[b]	$\Sigma\,\delta_{LE}$[c]	R	$\Sigma\,\delta_{LE}$	R	$\Sigma\,\delta_{LE}$
Bcl-xl (3spf)	0.56	14.78	0.71	11.85	0.85	7.32
Tubulin (4eb6)	0.61	14.52	0.51	11.85	0.18	7.33
FTase (1ld8)	0.65	12.97	0.62	10.56	0.61	6.49
NQO1 (2f1o)	0.62	12.92	0.76	10.43	0.43	6.43
Akt1 (3qkl)	0.80	10.93	0.64	8.89	0.20	5.53
c-Met (2wgj)	0.66	10.22	0.78	8.16	0.45	5.08
Bcl-2 (4aq3)	0.44	9.76	0.46	7.83	0.84	4.85
CDK2 (2w1h)	0.55	9.61	0.49	7.80	0.38	4.79
FAK1 (3bz3)	0.69	8.82	0.82	7.12	0.53	4.40
HSP90 (2wi6)	0.51	8.64	0.68	6.96	0.57	4.25

[a]Target abbreviations used: Bcl-xl – Bcl-2-like protein 1; FTase – protein farnesyltransferase; NQO1 – NAD(P)H: quinone dehydrogenase 1; Akt1 – RAC-alpha serine/threonine-protein kinase; c-Met – hepatocyte growth factor receptor; Bcl-2 – apoptosis regulator Bcl-2; CDK2 – cyclin-dependent kinase 2; FAK1 – focal adhesion kinase 1; HSP90 – heat shock protein HSP 90-alpha; [b]R – correlation factor between docking scores and IC_{50}; [c]$\Sigma\delta_{LE}$ – sums of docking scores across all the active protoberberines

TABLE III. Vina docking scores for the studied protoberberines across the 10 highest ranked target proteins

Cmpd.	Bcl-xl (3spf)	Tubulin (4eb6)	FTase (1ld8)	NQO1 (2f1o)	Akt1 (3qkl)	c-Met (2wgj)	Bcl-2 (4aq3)	CDK2 (2w1h)	FAK1 (3bz3)	HSP90 (2wi6)
18b	–8.4	–7.6	–9.2	–7.5	–8.9	–9.9	–7.7	–9.8	–8.7	–8.2
19b	–8.4	–7.6	–9.3	–7.7	–8.9	–10.0	–7.7	–9.9	–8.8	–8.3
18a	–7.8	–8.1	–9.0	–6.7	–8.4	–8.8	–7.3	–9.1	–8.3	–7.5
19a	–7.8	–7.8	–9.0	–6.7	–8.7	–8.9	–7.6	–10.0	–8.6	–7.6
18c	–7.1	–7.5	–8.4	–6.5	–8.2	–8.8	–6.2	–8.9	–7.6	–7.6
19c	–7.4	–7.5	–8.9	–6.5	–8.7	–8.6	–7.0	–9.2	–8.2	–7.1
20b	–7.9	–8.0	–8.9	–7.2	–8.6	–9.0	–7.5	–10.5	–8.5	–7.9
20a	–7.8	–7.8	–9.2	–6.7	–8.3	–8.6	–7.3	–9.4	–8.3	–7.5
20c	–7.2	–7.3	–8.7	–6.6	–8.0	–8.4	–6.5	–9.0	–8.3	–7.3
25	–8.1	–8.8	–9.8	–7.5	–9.3	–9.8	–7.2	–10.4	–8.8	–7.9
26	–7.9	–8.8	–9.3	–7.6	–9.5	–9.9	–7.1	–10.5	–9.0	–7.9
11	–7.3	–7.0	–7.6	–5.9	–7.4	–8.7	–6.7	–8.5	–7.7	–6.8

The obtained results were analyzed with respect to the existing literature evidence on the mechanism of action of related compounds. Naturally occurring protoberberines are known to interact with a variety of molecular targets resulting in antiproliferative and pro-apoptotic effects. Berberine, the best studied representative of this compound class, exerts these effects in various tumour cell lines through increased formation of reactive oxygen species (ROS), downregulation of anti-apoptotic proteins such as Bcl-2 and Bcl-xl, induction of apoptosis through mitochondrial-caspase activation, interaction with DNA and RNAs and/or topoisomerase poisoning.[48,49] A closely related benzylisoquinoline alkaloid, sanguinarine, is further known to inhibit microtubule assembly and to

modulate the levels of a Bcl-2 protein family member.[50,51] Effects similar to those of berberine on mitochondrial membrane potential, caspase activation and Bcl-2 protein family members have also been described for berbamine and anonaine.[52–55] When considered in context of the biological profile of well characterized benzylisoquinoline alkaloids, the results of the present virtual target screening suggest a similar putative mechanism of action of the newly synthesised derivatives, but also provide a novel potential molecular basis for these effects. The cytotoxicity of the studied compounds in myelogenous leukaemia K562 cells was found to correlate best with the presumed binding affinities of these compounds to Akt1. This finding is consistent with experimental evidence suggesting that berberine inhibits Akt1 activity and favours its degradation and that this results in reduced tumour cell viability and induction of apoptosis.[56,57] The good correlation between the docking scores at NQO1 and FTase could be rationalized in terms of increased ROS formation that could result from the inhibition of these enzymes.[58–60] Increased ROS formation is a known effect of protoberberines that could contribute to cell death *via* multiple pathways. Furthermore, disruption of microtubule assembly could also contribute to cell-cycle arrest and induction of apoptosis, although this does not seem to be a major determinant of cytotoxicity in the FemX cell line. Conversely, interaction with Bcl-2 family proteins showed significant association with *in vitro* activity in FemX as well as the other two cell lines. As presented in Table III, most of the compounds that were found to be inactive in the HeLa and FemX cell lines have lower docking scores than the active protoberberines, although these differences are not large. These findings might be attributed to differential susceptibility of the tested cell lines to inhibition of the proposed putative targets, but also points to the fact that the developed compounds exhibit low specificity binding and lack significant potency at individual targets. To investigate the possibility of further structural optimization using the developed synthetic strategy, the molecular aspect of the interaction between the studied compounds and their likely targets was analysed. In terms of structural determinants of the observed activity, the interaction of the studied protoberberines with most of the identified putative targets is largely non-specific and governed by hydrophobic interactions. This is best exemplified by the proposed binding modes of the studied structures at the Bcl-xl protein. As shown in Fig. 5a, they occupy a hydrophobic pocket which is also exploited by a potent small molecule inhibitor BM501.[61] Lacking any strictly directional interactions with the binding site residues, compounds **18b**, **20c** and **25**, shown in Fig. 5a as representative structures, differ in their binding modes largely due to differences in size and polarity. The smallest, least polar and most potent of them, **18b**, is able to localize deep in the binding pocket, whereas the increased size and polarity of the other two compounds allow them to fit only partially into the deep pocket, with reduced binding affinity as a con-

sequence. Some of the other potential targets, on the other hand, seem to show a greater tolerance for variations in size and interact more favourably with the extended structures. In the instance of binding to the vinblastine related site at the heterodimeric interface of tubulin (Fig. 5b), **25** shows the highest target affinity due to a greater number of hydrophobic contacts as opposed to **18a** and **18b**.

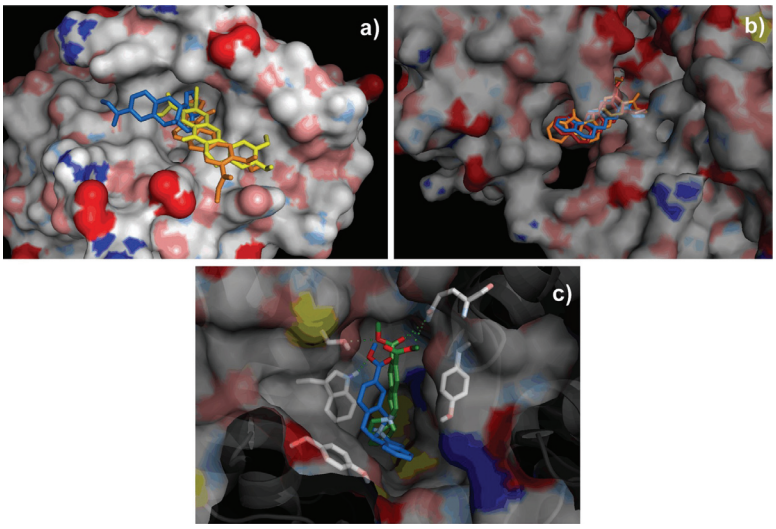

Fig. 5. Binding modes at: a) Bcl-xl (PDB: 3spf), **18b** (blue), **25** (orange), **20c** (yellow); b) tubulin (PDB: 4eb6), **18b** (blue), **18a** (red), **25** (orange); c) FTase (PDB1ld8), **18b** (blue), **18a** (green).

As exemplified by the differences in docking scores between the latter two closely related structures (Table III, –8.1 and –7.6, respectively), variation of substituents in ring D, easily accessible by the developed synthetic route, could present the basis for improving the affinity and specificity in targeting tubulin. While C11 carboxyl substituents might cause steric hindrance, variation of C10 substituents is likely to allow the exploration of the deep adjacent pocket and increase specificity through H-bonding. The potential usefulness of varying these substituents is also exemplified by the putative binding modes of **18a** and **18b** in the FTase active site, as illustrated in Fig. 5c. The presence and nature of these substituents seem to play noteworthy roles in the orientation of the relatively rigid polycyclic core in the binding sites, which consequently affects the extent of hydrophobic contacts made with the protein. The overall observations suggest that careful variation of these substituents could impart target selectivity to an otherwise promiscuous compound class and that it could potentially present the basis for advancing the multi-targeted mechanism of action of naturally occurring or synthesised protoberberines to a more specific one. Further biochemical profiling of activity on these targets is therefore highly warranted.

EXPERIMENTAL

Chemistry

General. The NMR spectra were recorded on a Bruker Avance III (500 MHz) or Varian Gemini 2000 (200 MHz) spectrometers. Chemical shifts (δ) are given in ppm downfield from tetramethylsilane as the internal standard. Deuterochloroform was used as the solvent, unless otherwise stated. Mass spectral data were recorded using an Agilent MSD TOF spectrometer coupled with Agilent 1200 HPLC or an Agilent Technologies 5975C MS coupled with an Agilent Technologies 6890N GC. The IR spectra were recorded on an IR Thermo Scientific Nicolet iS10 (4950) spectrometer. Melting points were determined using a Gallenkamp melting point apparatus and are uncorrected. Flash chromatography employed silica gel 60 (230–400 mesh) while thin layer chromatography was performed using alumina plates with a 0.25 mm silica layer (Kieselgel 60 F_{254}, Merck). The compounds were visualised by staining with potassium permanganate solution or Dragendorff reagent. All solvents were distilled before the use. Petroleum ether refers to fraction boiling in the 40–60 °C range.

Spectral data for the synthesised compounds and selected NMR spectra are given in Supplementary material to this paper.

Synthetic procedures

3,4-Dihydro-β-carboline, 6,7-dimethoxyisoquinoline and 3-bromo-2-iodoprop-1-ene were synthesised following literature procedures.[62-64]

General procedure for the preparation of iminium salts. Heterocyclic compound (2.5 mmol; isoquinoline, 3,4-dihydro-β-carboline, pyridine) and 3-bromo-2-halogenprop-1-ene (1.1 eq) were heated in acetonitrile (10 mL) at 80 °C for 4 h. The mixture was then cooled to room temperature, the acetonitrile was removed under reduced pressure and the crude salt was washed with dry diethyl ether (3×5 mL). The product was dried under reduced pressure at room temperature. The synthesised salts were used in the next step without further characterisation.

General procedure for the addition of allylmagnesium bromide to the iminium salts. Magnesium turnings (1.06 g, 44 mmol) were added to a two-necked round-bottom flask assembled with a reflux condenser, which had been flame dried and allowed to cool under a stream of nitrogen. Dry diethyl ether (5 mL) was added to flask under stirring. Then, the round-bottom flask was cooled to 0 °C in an ice bath. A solution of allyl bromide (4.84 g, 40 mmol, 3.4 mL) in dry diethyl ether (40 mL) was slowly added to the flask and the reaction mixture was stirred for 1 h at room temperature. The iminium salt (16 mmol) was then added to solution of Grignard reagent and reaction mixture was stirred for 1 h at room temperature. Excess of allylmagnesium bromide was destroyed with a saturated solution of ammonium sulphate at 0 °C. The organic layer was separated and aqueous layer was extracted with diethyl ether (2×25 mL). The combined organic layers were dried over anhydrous sodium sulphate. After filtration and removal of the solvent under reduced pressure, the crude enamine was reduced without prior purification.

General procedure for the reduction of enamines. A crude enamine (1.2 mmol) was dissolved in dry MeOH (5 mL) and cooled under stirring to 0 °C. Sodium cyanoborohydride (3.6 mmol) was then added, and the suspension was acidified with concentrated HCl to pH close to 3. The resulting mixture was allowed to warm to room temperature and stirring was continued for 4 h. 1M NaOH was then added until pH close to 10, the mixture was extracted with dichloromethane (3×30 mL), the combined organic layers were washed with water (2×5 mL)

and dried over anhydrous sodium sulphate. After filtration and removal of the solvent, the residue was evaporated under reduced pressure and purified by flash chromatography (SiO_2).

General procedure for the synthesis of dienes. A mixture of halogenalkene (0.7 mmol), $Pd(OAc)_2$ (10 mol %), PPh_3 (20 mol %) and K_2CO_3 (1.5 eq.) in acetonitrile (10 mL) was refluxed under a nitrogen atmosphere for 12 h. After evaporation *in vacuo*, the residue was dissolved in dichloromethane, washed with water and dried over anhydrous sodium sulphate. The solid was separated by filtration and the solvent removed under reduced pressure. The residue was purified by flash chromatography (SiO_2) to afford the product.

General procedure for the synthesis of cycloadducts. A mixture of diene (0.2 mmol) and dienophile (0.24 mmol) in dry toluene (5 mL) was refluxed under a nitrogen atmosphere for 12 h. The solvent was then evaporated under reduced pressure and the residue was purified by flash chromatography (SiO_2) to afford the product.

General procedure for the synthesis of tetrahydroprotoberberines. A mixture of cycloadduct (0.1 mmol) and MnO_2 (2.2 mmol) in dry dichloromethane (20 mL) was stirred and refluxed under a nitrogen atmosphere. The reaction was monitored by TLC and when completed (≈30 min), the mixture was cooled to room temperature, diluted with dichloromethane (20 mL) and filtered through a pad of celite. The pad was rinsed until the filtrate was colourless. The solvent was then evaporated under reduced pressure and the residue was purified by flash chromatography (SiO_2). Tetrahydroprotoberberines give an orange-red colour with Dragendorff reagent.

General procedure for the synthesis of 8-oxoprotoberberines. A mixture of cycloadduct (0.1 mmol) and MnO_2 (10 mmol) in dry dichloromethane (20 mL) was stirred and refluxed under nitrogen atmosphere for 24 h. The reaction mixture was cooled to room temperature, diluted with dichloromethane (20 mL) and filtered through a pad of celite. The colour of filtrate was fluorescent yellow. The celite pad was rinsed with ethyl acetate until the filtrate was colourless. The solvent was then evaporated under reduced pressure and the residue was purified by flash chromatography (SiO_2). 8-Oxoprotoberberines give specific colours with Dragendorff reagent.

Biology

Cell culture. Human cervix adenocarcinoma (HeLa) and human melanoma (Fem-x) cells were cultured as monolayers. Human chronic myelogenous leukaemia (K562) cells were grown in a suspension in nutrient medium. The cancer cell lines were obtained from the American Type Culture Collection (Manassas, VA, USA). The complete nutrient medium was RPMI 1640 supplemented with 3 mM L-glutamine, 100 μg mL^{-1} streptomycin, 100 IU mL^{-1} penicillin, 10 % heat-inactivated (56 °C) foetal bovine serum and 25 mM Hepes adjusted to pH 7.2 with a bicarbonate solution. The cells were grown at 37 °C in an atmosphere of 5 % CO_2 and humidified air. RPMI 1640, L-glutamine and Hepes were obtained from PAA (Pasching, Austria).

Cell sensitivity analysis. The HeLa and Fem-x cells were seeded (2000 cells per well) into 96-well microtiter plates, and 20 h later, after cell adherence, five different concentrations of the test compounds were added to different wells. The final concentrations of the test compounds were from 12.5 to 200 μM. Only nutrient medium was added to the cells in the control wells. For the K562 cells, the test compounds were added to cell suspensions (3000 cells per well) 2 h after cell seeding, at the same final concentrations as applied to the HeLa and Fem-x cells. All of the experiments were performed in triplicate. Nutrient medium with the corresponding concentrations of the test compounds, but void of cells, was used as the blank. Cisplatin was used as a positive control.

Determination of target-cell survival. Cell survival was determined by the 3-(4,5-dimethylthiazol-2-yl)-2,5-diphenyltetrazolium bromide (MTT) test according to the method of Mosmann[65] and modified by Ohno and Abe.[66] Briefly, 20 μL MTT solution (5 mg mL^{-1} in phosphate buffered saline) was added to each well. The samples were incubated for a further 4 h at 37 °C in 5 % CO_2 with a humidified atmosphere. Then, 100 mL 10 % sodium dodecyl sulphate (SDS) was added to each of the wells, and the absorbance of the cell medium from each well was measured at 570 nm the next day. To calculate the cell survivals (%), the absorbance at 570 nm of each of the samples with cells grown in the presence of the test compounds were divided by the absorbance of the control sample (the absorbance of cells grown in nutrient medium only), after the subtraction of the blank sample absorbance. The IC_{50} was defined as the concentration of the agent that inhibited cell survival by 50 %, compared to the vehicle-treated control.

Cell cycle analysis. The cellular DNA content and cell distribution were quantified by flow cytometry using propidium iodide (PI). HeLa cells were incubated in the presence of two different concentrations (corresponding to the IC_{50} and IC_{90} values determined after 72 h) of the examined compounds for 24 h. After these incubation times, the target cells were collected, washed and fixed in 70 % ethanol on ice. The samples were stored at –20 °C for one week before staining. The HeLa cells were washed in PBS, resuspended in 500 μL of staining solution (PBS containing RNAse A at a final concentration of 200 μg mL^{-1}, and propidium iodide (PI) at a final concentration of 20 μg mL^{-1}), and incubated for 30 min at 37 °C. The cell cycle phase distribution was determined using a FACSCalibur Flow Cytometer (BD Biosciences, Franklin Lakes, NJ, USA). The data (10,000 events collected for each sample) were analyzed using CELLQuest software (BD Biosciences).[67]

Morphological evaluation of HeLa cell death. Morphological features of HeLa cell death induced by investigated compounds were analyzed after staining the treated cells with a mixture of acridine orange (AO) and ethidium bromide (EB).[68] Briefly, 1×10^5 HeLa cells were seeded on a glass slide in Petri dishes, and treated the next day with $2\times IC_{50}$ concentration of the investigated compounds for 24 h. Then, the cells were stained with 15 μL of a mixture of the working concentration of AO/EB (3 μg mL^{-1} AO and 10 μg mL^{-1} EB in phosphate buffered saline (PBS) and visualized under a fluorescence microscope using a fluorescein isothiocyanate (FITC) filter set.

Computational chemistry

Ligand preparation. Structures of the 12 biologically evaluated protoberberines were modelled in MarvinSketch 5.10.1[69] and saved in MDL .mol format. To determine the protonation state of the studied compounds for docking studies, the pK_a values were predicted using the corresponding MarvinSketch plugin. All of the modelled structures were further processed in Vega ZZ 3.0.[70,71] SP4 atom types and Gasteiger charges were assigned before running an AMMP systematic conformational search involving all flexible torsions, with 10 steps per torsion and a 100 step conjugate gradients minimization of each generated conformation. The lowest energy conformer for each structure was saved in .mol2 format and prepared for docking studies using AutoDock Tools 1.5.6,[72] whereby .pdbqt ligand files were generated. All flexible torsions were retained as active.

Target pool construction and receptor files preparation. A set of 126 antitumour-related targets previously compiled and used in inverse docking studies[73] served as the basis for the target pool used in this study. Online server idTarget[74] was used to preliminary identify a subset of the 126 targets with which the most potent of the studied protoberberines (**18b**) could favourably interact. As the aim of the virtual screening was to rationalize the mech-

anism of the observed antiproliferative activity, targets the inhibition of which could not account for the cell cycle arrest and induction of apoptosis observed in the studied cell lines (*e.g.*, matrix metalloproteinases, some cathepsins) were excluded to refine the target pool. Additionally, a literature search was conducted to identify targets that had previously been implicated in the mode of action of naturally occurring and synthetically derived protoberberines and related structures. These targets were used to expand the initial subset if their crystallographic structures were available. In total, 58 targets were screened with multiple pdb entries for some proteins.

The structures of all the macromolecules in the final target pool were downloaded from the Protein Data Bank and processed in AutoDock Tools by removing water molecules and co-crystallized ligands, adding polar hydrogens and assigning Gasteiger charges. The receptors were treated as rigid. The centres of the grid box for the docking studies were defined with respect to the spatial centre of the co-crystallized ligand. For most receptors, the grid box dimensions were 18 Å×18 Å×18 Å which allowed for free rotation of all the studied protoberberine structures and completely covered the binding site of the co-crystallized ligand. If the binding site extended beyond these dimensions, the grid box was enlarged correspondingly.

Virtual screening. Docking of the 12 biologically evaluated protoberberines against the final pool of targets was performed using AutoDock Vina[75] and AUDocker LE as a graphical user interface facilitating virtual screening applications of AutoDock Vina.[76] The level of exhaustiveness was set at 16 while the remaining Vina docking parameters were retained at their default values. Ten independent runs were performed for both protonated and neutral forms of all the ligands and the mean values of the docking scores corresponding to the lowest energy binding mode were saved for further analysis. For ligands whose pK_a values would allow both ionized and neutral species to exist at the physiological pH of 7.4, the docking scores corresponding to the energetically more favourable interaction with each target were chosen.

As it was previously demonstrated that unprocessed docking scores against a set of various protein structures do not reveal the most likely putative targets, the prioritization of virtual screening hits was based on how well the obtained arrays of binding energies correspond to *in vitro* activity. To determine this, mean docking scores and IC_{50} values for all compounds that were considered active in the MTT test ($IC_{50} \leq 150$ μM) were imported into RapidMiner 5[77] and a correlation matrix was calculated. Pairwise correlation coefficients for each cell line and putative targets were ranked in descending order and analyzed. To further refine the results, the 10 targets with the highest correlation coefficients were chosen and their co-crystallised ligands were docked using previously described procedures to obtain the AutoDock Vina docking scores. These results were then used to compute normalized docking results based on ligand efficiencies,[78,79] as presented in Eq. (1) and as previously described:[73]

$$\delta_{LE} = \frac{LE_{\mathrm{LIG}}}{LE_{\mathrm{REF}}} = \frac{\Delta G_{\mathrm{LIG}} / N_{\mathrm{LIG}}}{\Delta G_{\mathrm{REF}} / N_{\mathrm{REF}}} \quad (1)$$

where δ_{LE} represents the normalized docking score, *LE* the ligand efficiency for the screened ligand (LIG) *versus* the *LE* of the co-crystallised (REF) ligand, calculated by dividing the corresponding docking scores (ΔG) by the number of non-hydrogen atoms (N) in the respective compound. Targets with the higher sum of δ_{LE} for the active compounds were prioritized over those with lower sums of the normalized docking scores.

CONCLUSIONS

A series of novel protoberberine-like compounds were synthesised and their anticancer potential was displayed on K562, HeLa and FemX cell lines. Further computational exploration provided insight into the potential mechanism of their action, suggesting that they probably act through multiple pathways. Several putative biological targets for these molecules were recognized while a docking study indicated possible directions for their further derivatisation, favouring modifications of the terminal ring D. The outlined synthesis provides control over the substitution pattern of the ring D and this potential combined with functionalised heterocycles, as starting materials, bearing substituted ring A, may provide access to a wider range of protoberberine-inspired compounds. Based on the presented results, it is believed that the flexibility of the synthetic route associated with results of the computational study may lead to rationally designed compounds with significantly improved potency and selectivity profiles, work that is presently ongoing.

SUPPLEMENTARY MATERIAL

Spectral data for synthesised compounds and copies of selected NMR spectra are available electronically from http://www.shd.org.rs/JSCS/, or from the corresponding author on request.

Acknowledgements. Financial support from the Serbian Ministry of Education, Science and Technological Development (Grants 172009 and 175011) is greatly appreciated.

ИЗВОД

СИНТЕЗА, ЦИТОТОКСИЧНОСТ И РАЧУНАРСКА СТУДИЈА НОВИХ ПРОТОБЕРБЕРИНСКИХ ДЕРИВАТА

МИЛЕНА Р. СИМИЋ[1], АНА Б. ДАМЈАНОВИЋ[2], МАРКО Д. КАЛИНИЋ[3], ГОРДАНА Д. ТАСИЋ[1], СЛАВИЦА М. ЕРИЋ[3], ЈЕЛЕНА А. АНТИЋ-СТАНКОВИЋ[4] и ВЛАДИМИР М. САВИЋ[1]

[1]Универзитет у Београду, Фармацеутски факултет, Катедра за органску хемију, Војводе Степе 450, 11221 Београд, [2]Институт за онкологију и радиологију, Одељење за експерименталну онкологију, Пастерова 14, 11000 Београд, [3]Универзитет у Београду, Фармацеутски факултет, Катедра за фармацеутску хемију, Војводе Степе 450, 11221 Београд и [4]Универзитет у Београду, Фармацеутски факултет, Катедра за имунологију и микробиологију, Војводе Степе 450, 11221 Београд

Развијен је нов и ефикасан синтетски пут за добијање протоберберинских деривата. Ова методологија, базирана пре свега на супституцији крајњег прстена, примењена је за добијање мале серије ових једињења. Њихово почетно биолошко профилисање указало је на антипролиферативни потенцијал. Рачунарским методама идентификована су потенцијална циљна места дејства и установљена рационална основа за даље структурне модификације. Иако активност синтетисаних деривата захтева додатно унапређење, ова студија је показала да описани приступ може бити користан у креирању нових водећих молекула.

(Примљено 25. маја, ревидирано 19. октобра, прихваћено 26. октобра 2015)

REFERENCES

1. K. C. Morrison, P. J. Hergenrother, *Nat. Prod. Rep.* **31** (2014) 6
2. D. J. Newman, G. M. Cragg, *J. Nat. Prod.* **75** (2012) 311
3. B. K. Shoichet, *Nat. Chem.* **5** (2012) 9
4. B. B. Mishra, V. K. Tiwari, *Eur. J. Med. Chem.* **46** (2011) 4769
5. I. Vetter, J. L. Davis, L. D. Rash, R. Anangi, M. Mobli, P. F. Alewood, R. J. Lewis, G. F. King, *Amino Acids* **40** (2011) 15
6. A. L. Harvey, R. L. Clark, S. P. Mackay, B. F. Johnston, *Expert Opin. Drug Discov.* **5** (2010) 559
7. T. F. Molinski, D. S. Dalisay, S. L. Lievens, J. P. Saludes, *Nat. Rev. Drug Discov.* **8** (2009) 69
8. J. W.-H. Li, J. C. Vederas, *Science* **325** (2009) 161
9. T. Beghyn, R. Deprez-Poulain, N. Willand, B. Folleas, B. Deprez, *Chem. Biol. Drug Des.* **72** (2008) 3
10. A. Saklani, S. K. Kutty, *Drug Discov. Today* **13** (2008) 161
11. J. P. Nandy, M. Prakesch, S. Khadem, P. T. Reddy, U. Sharma, P. Arya, *Chem. Rev.* **109** (2009) 1999
12. S. Rizzo, H. Waldmann, *Chem. Rev.* **114** (2014) 4621
13. H. Lachance, S. Wetzel, K. Kumar, H. Waldmann, *J. Med. Chem.* **55** (2012) 5989
14. E. Reimann, *Curr. Org. Chem.* **13** (2009) 353
15. L. Grycová, J. Dostál, R. Marek, *Phytochemistry* **68** (2007) 150
16. E. V. Leitao da-Cunha, I. M. Fechine, D. N. Guedes, J. M. Barbosa-Filho, M. Sobral da Silva, *Alkaloids: Chem. Biol.* **62** (2005) 1
17. K. Bhadra, M. Maiti, G. S. Kumar, *Chem. Biodiversity* **6** (2009) 1323
18. P. Giri, M. Hossain, G. S. Kumar, *Int. J. Biol. Macromol.* **39** (2006) 210
19. M. Sanders, A. Liu, T.-K. Li, H.-Y. Wu, S. Desai, Y. Mao, E. Rubin, E. LaVoie, D. Makhey, L. Liu, *Biochem. Pharmacol.* **56** (1998) 1157
20. S. A. Kim, Y. Kwon, J. H. Kim, M. T. Muller, I. K. Chung, *Biochemistry (Moscow)* **37** (1998) 16316
21. C. Kan-Fan, H.-P. Husson, *Tetrahedron Lett.* **21 (**1980) 1463
22. A. Le Hir, R. Goutarel, M.-M. Janot, A. Hofmann, *Helv. Chim. Acta* **37** (1954) 2161
23. D. E. Larsson, S. B. Hassan, K. Oberg, D. Granberg, *Anti-Cancer Agents Med. Chem.* **12** (2012) 783
24. K. H. Kim, I. K. Lee, C. J. Piao, S. U. Choi, J. H. Lee, Y. S. Kim, K. R. Lee, *Bioorg. Med. Chem. Lett.* **20** (2010) 4487
25. J. Liang, C. Woodward, H. Edelsbrunner, *Protein Sci.* **7** (1998) 1884
26. S. Husinec, V. Savic, M. Simic, V. Tesevic, D. Vidovic, *Tetrahedron Lett.* **52** (2011) 2733
27. D. Barbier, C. Marazano, C. Riche, B. C. Das, P. Potier, *J. Org. Chem.* **63** (1998) 1767
28. P. D. Baird, J. Blagga, S. G. Davies, K. H. Sutton, *Tetrahedron* **44** (1988) 171
29. L. A. T. Cleghorn, R. Grigg, C. Kilner, W. S. MacLachlan, V. Sridharan, *Chem. Commun.* (2005) 3071
30. J. T. Link, *Org. React. (Hoboken, NJ, U.S.)* **60** (2004) 157
31. R. Grigg, P. Stevenson, T. Worakun, *Tetrahedron* **44** (1988) 2049
32. J. Baran, H. Mayr, *Tetrahedron* **45** (1989) 3347
33. W. F. Bailey, N. M. Wachter-Jurcsak, M. R. Pineau, T. V. Ovaska, R. R. Warren, C. E. Lewis, *J. Org. Chem.* **61** (1996) 8216
34. G. Burnier, L. Schwager, P. Vogel, *Helv. Chim. Acta* **69** (1986) 1310

35. S. Pujari, K. Kaliappan, A. Valleix, D. Grée, R. Grée, *Synlett* (2008) 2503
36. S. Kotha, P. Khedkar, *J. Org. Chem.* **74** (2009) 5667
37. J. J. Vanden Eynde, F. Delfosse, A. Mayence, Y. Van Haverbeke, *Tetrahedron* **51** (1995) 6511
38. U. Ziegler, P. Groscurth, *Physiology* **19** (2004) 124
39. J. L. Jenkins, A. Bender, J. W. Davies, *Drug Discov. Today: Technol.* **3** (2006) 413
40. A. Koutsoukas, B. Simms, J. Kirchmair, P. J. Bond, A. V. Whitmore, S. Zimmer, M. P. Young, J. L. Jenkins, M. Glick, R. C. Glen, A. Bender, *J. Proteomics* **74** (2011) 2554
41. D. Rognan, *Mol. Inf.* **29** (2010) 176
42. E. Kellenberger, N. Foata, D. Rognan, *J. Chem. Inf. Model.* **48** (2008) 1014
43. Y. Y. Li, J. An, S. J. M. Jones, *PLoS Comput. Biol*. **7** (2011) e1002139.
44. G. P. A. Vigers, J. P. Rizzi, *J. Med. Chem.* **47** (2004) 80
45. D. N. Santiago, Y. Pevzner, A. A. Durand, M. Tran, R. R. Scheerer, K. Daniel, S.-S. Sung, H. Lee Woodcock, W. C. Guida, W. H. Brooks, *J. Chem. Inf. Model.* **52** (2012) 2192
46. J. W. M. Nissink, *J. Chem. Inf. Model.* **49** (2009) 1617
47. M. Jacobsson, A. Karlén, *J. Chem. Inf. Model*. **46** (2006) 1334
48. M. Tillhon, L. M. Guamán Ortiz, P. Lombardi, A. I. Scovassi, *Biochem. Pharmacol.* **84** (2012) 1260
49. Y. Sun, K. Xun, Y. Wang, X. Chen, *Anticancer Drugs* **20** (2009) 757
50. M. Lopus, D. Panda, *FEBS J.* **273** (2006) 2139
51. H. Ahsan, S. Reagan-Shaw, J. Breur, N. Ahmad, *Cancer Lett.* **249** (2007) 198
52. Y.-L. Wei, Y. Liang, L. Xu, X.-Y. Zhao, *Anat. Rec.* **292** (2009) 945
53. Y. Wei, L. Xu, Y. Liang, X. Xu, X. Zhao, *Acta Pharmacol. Sin.* **30** (2009) 451
54. R. Xu, Q. Dong, Y. Yu, X. Zhao, X. Gan, D. Wu, Q. Lu, X. Xu, X.-F. Yu, *Leuk. Res.* **30** 2006 17
55. C.-Y. Chen, T.-Z. Liu, W.-C. Tseng, F.-J. Lu, R.-P. Hung, C.-H. Chen, C.-H. Chen, *Food Chem. Toxicol.* **46** (2008) 2694
56. N. Wang, Y. Feng, M. Zhu, C.-M. Tsang, K. Man, Y. Tong, S.-W. Tsao, *J. Cell. Biochem.* **111** (2010) 1426
57. H.-P. Kuo, T.-C. Chuang, S.-C. Tsai, H.-H. Tseng, S.-C. Hsu, Y.-C. Chen, C.-L. Kuo, Y.-H. Kuo, J.-Y. Liu, M.-C. Kao, *J. Agric. Food. Chem.* **60** (2012) 9649
58. D. N. Criddle, S. Gillies, H. K. Baumgartner-Wilson, M. Jaffar, E. C. Chinje, S. Passmore, M. Chvanov, S. Barrow, O. V. Gerasimenko, A. V. Tepikin, R. Sutton, O. H. Petersen, *J. Biol. Chem.* **281** (2006) 40485
59. J. Pan, M. She, Z.-X. Xu, L. Sun, S.-C. J. Yeung, *Cancer Res.* **65** (2005) 3671
60. J. Pan, S.-C. J. Yeung, *Cancer Res.* **65** (2005) 9109
61. H. Zhou, J. Chen, J. L. Meagher, C.-Y. Yang, A. Aguilar, L. Liu, L. Bai, X. Cong, Q. Cai, X. Fang, J. A. Stuckey, S. Wang, *J. Med. Chem.* **55** (2012) 4664
62. N. Whittaker, *J. Chem. Soc., C* (1969) 85
63. A. Metzger, M. A. Schade, P. Knochel, *Org. Lett.* **10** (2008) 1107
64. M. Kurosu, M.-H. Lin, Y. Kishi, *J. Am. Chem. Soc.* **126** (2004) 12248
65. T. Mosmann, *J. Immunol. Methods* **65** (1983) 55
66. M. Ohno, T. Abe, *J. Immunol. Methods* **145** (1991) 199
67. R. H. Clothier, in In Vitro *Toxicity Testing Protocols*, S. O'Hare, C. K. Atterwill, Eds., Humana Press, Totowa, NJ, 1995, p. 109
68. N. K. Banda, W. C. Satterfield, A. Dunlap, K. S. Steimer, R. Kurrle, T. H. Finkel, *Apoptosis* **1** (1996) 49

69. *MarvinSketch 5.10.1*, ChemAxon, 2012
70. A. Pedretti, L. Villa, G. Vistoli, *J. Comput.-Aided Mol. Des.* **18** (2004) 167
71. A. Pedretti, L. Villa, G. Vistoli, *J. Mol. Graphics Modell.* **21** (2002) 47
72. G. M. Morris, R. Huey, W. Lindstrom, M. F. Sanner, R. K. Belew, D. S. Goodsell, A. J. Olson, *J. Comput. Chem.* **30** (2009) 2785
73. G. Lauro, A. Romano, R. Riccio, G. Bifulco, *J. Nat. Prod.* **74** (2011) 1401
74. J.-C. Wang, P.-Y. Chu, C.-M. Chen, J.-H. Lin, *Nucleic Acids Res.* **40** (2012) W393
75. O. Trott, A. J. Olson, *J. Comput. Chem.* **31** (2010) 455
76. G. Sandeep, K. P. Nagasree, M. Hanisha, M. M. K. Kumar, *BMC Res. Notes* **4** (2011) 445
77. *RapidMiner version 5.2*, Rapid-I GmbH, Dortmund, Germany, 2012.
78. C. Abad-Zapatero, J. T. Metz, *Drug Discov. Today* **10** (2005) 464
79. A. L. Hopkins, C. R. Groom, A. Alex, *Drug Discov. Today* **9** (2004) 430.